npg

Growth differentiation factor-15 encodes a novel microRNA 3189 that functions as a potent regulator of cell death

MF Jones[1,7], X Ling Li[1,7], M Subramanian[1,7], Svetlana A Shabalina[2], T Hara[1], Y Zhu[3], J Huang[4], Y Yang[5], LM Wakefield[5], KV Prasanth[6] and A Lal*,[1]

According to the latest version of miRBase, approximately 30% of microRNAs (miRNAs) are unique to primates, but the physiological function of the vast majority remains unknown. In this study, we identified miR-3189 as a novel, p53-regulated, primate-specific miRNA embedded in the intron of the p53-target gene *GDF15*. Antagonizing miR-3189 increased proliferation and sensitized cells to DNA damage-induced apoptosis, suggesting a tumor suppressor function for endogenous miR-3189. Identification of genome-wide miR-3189 targets revealed that miR-3189 directly inhibits the expression of a large number of genes involved in cell cycle control and cell survival. In addition, miR-3189 downregulated the expression of multiple p53 inhibitors resulting in elevated p53 levels and upregulation of several p53 targets including p21 (*CDKN1A*), *GADD45A* and the miR-3189 host gene *GDF15*, suggesting miR-3189 auto-regulation. Surprisingly, miR-3189 overexpression in p53-/- cells upregulated a subset of p53-targets including *GDF15*, *GADD45A*, and *NOXA*, but not *CDKN1A*. Consistent with these results, overexpression of miR-3189 potently induced apoptosis and inhibited tumorigenicity *in vivo* in a p53-independent manner. Collectively, our study identified miR-3189 as a novel, primate-specific miRNA whose effects are mediated by both p53-dependent and p53-independent mechanisms. miR-3189 may, therefore, represent a novel tool that can be utilized therapeutically to induce a potent proapoptotic effect even in p53-deficient tumors.

Cell Death and Differentiation (2015) 22, 1641–1653; doi:10.1038/cdd.2015.9; published online 20 February 2015

MicroRNAs (miRNAs) are short, 18–22 nucleotide (nt) non-coding RNAs that play important roles in regulating the expression of protein-coding genes. MiRNAs primarily bind to partially complementary sites in the 3′ untranslated region (UTR) of target mRNAs,[1,2] inducing translation inhibition and/or mRNA degradation.[3] They have been implicated in a wide range of cellular processes from embryogenesis to tumor suppression. Aberrant miRNA expression is a molecular genetic feature of many cancers,[4,5] and miRNAs are often globally downregulated in tumors.[6] The transcription factor and tumor suppressor p53 has been extensively studied as a regulator of miRNA expression.[7,8] Many miRNAs are transcriptionally regulated by p53 and modulate cell proliferation, stress response, differentiation and a host of other programs associated with p53 activation.[9] For instance, p53 has been shown to transactivate miR-34a after DNA damage, and miR-34a, in turn, represses the expression of pro-proliferative genes including *MYC*, *CDK6*, *CCNA1* and *HDM4*.[10–14]

Several p53-responsive miRNAs are intragenic and transcriptionally co-regulated with their host genes, such as miR-107/*PANK1*[15] and miR-29/*PINT*.[16,17] Recent high-throughput RNA sequencing studies have provided evidence supporting the existence of another such miRNA, the putative miR-3189,[18,19] embedded in the intron of the p53-inducible [20] TGF-*β* superfamily member[21] *GDF15* on chromosome 19p13.11. Although these studies indicated the production of a short, non-coding transcript that aligns to the intron of *GDF15*, it is not clear whether this transcript produces a functional miRNA.

The traditional argument supporting non-coding RNA function invokes evolutionary conservation to justify physiological relevance,[22] yet a growing number of poorly conserved miRNAs have been identified in human cells: ~30% of the miRNAs in the most recent version of miRBase (Release 20) are unique to primates. However, the proportion of primate-specific miRNA precursors that produce mature miRNAs remains unknown. Among the few primate-specific miRNAs that have been studied, miR-4423 was recently shown to mediate airway epithelial differentiation in the lung and suppress tobacco-associated carcinogenesis.[23] The miR-548 family is conserved only among primates,[24] yet has significant effects on tumorigenicity and angiogenesis.[25] Here, we

identify miR-3189 as a miRNA produced through canonical miRNA biogenesis pathways and conserved between humans and old-world apes. Furthermore, we characterize miR-3189 as a novel p53-regulated miRNA, an important component of the cellular response to DNA damage, and a potent effector of cell death in cancer cells irrespective of p53 mutation status.

Results

miR-3189 is a miRNA embedded in the intron of the p53 target gene *GDF15*.

The putative miR-3189 stem-loop sequence is located within the only intron of *GDF15*, roughly 100 bp from the 5′ splice site (Figure 1a). In an unpublished microarray study, we evaluated changes in mRNA and long non-coding RNA expression following induction of p53 by treatment with the MDM2 inhibitor Nutlin-3 in the p53 wild-type HCT116, RKO and SW48 colorectal cancer cell lines (Supplementary Figure S1). The results of this array indicated that the miR-3189 primary transcript (pri-miR-3189) was strongly upregulated in response to p53 activation in all three lines (Subramanian *et al.*, manuscript in preparation).

The human miR-3189 precursor (pre-miR-3189) is highly conserved in apes and old-world monkeys (*Catarrhini*) and is predicted to fold into a stable, conserved miRNA-like structure in these species (Figure 1b and c). Orthologous candidates of miR-3189 in distantly related primates (new-world monkeys) and other mammals are less conserved and are not predicted to form miRNA-like stable hairpins (Supplementary Figure S2 and S3), although genomic alignment of these regions is clearly syntenic (data not shown). Recent studies have implicated primate-specific miRNAs in several important physiological processes.[23,26] Because *GDF15* is a target of p53, we hypothesized that the embedded miR-3189 is also p53-responsive. Indeed, the pattern of pri-miR-3189 expression closely matched that of its host gene following p53 activation. We observed increased levels of both *GDF15* mRNA (>eightfold) and pri-miR-3189 (>sevenfold) by quantitative reverse transcription PCR (RT-qPCR) upon activation of p53 by Nutlin-3 in all three colorectal cancer lines (Figure 1d). To ascertain the involvement of miR-3189 in the p53-mediated DNA damage response, we treated HCT116 cells with a sub-lethal dose of the DNA damaging agent Doxorubicin (Dox, 300 nM) and measured changes in GDF15 and pri-miR-3189 by RT-qPCR. The levels of *GDF15* mRNA and pri-miR-3189 increased within 4 h of Dox treatment (Figure 1e).

The existing annotation of miR-3189 relies exclusively on mapping of RNA-seq reads, so we sought to confirm that the *GDF15* locus produces a mature miRNA. We therefore cloned the predicted stem-loop sequence of miR-3189 into a lentiviral expression vector (pCDH). Transfection of this pri-miR-3189 construct in HCT116 cells resulted in upregulation of the predicted mature products miR-3189-3p (~30-fold) and miR-3189-5p (~8-fold) but not the unrelated miR-34a (Figure 1f), suggesting that miR-3189-3p is the major miRNA produced from the *GDF15* locus. We therefore decided to study miR-3189-3p in more detail. Mature miR-3189-3p was upregulated when HCT116 cells were treated with Nutlin-3 or Dox (Figure 1g). miR-34a was included as a positive control. Immunoprecipitation (IP) of the RNA-induced silencing complex (RISC) with anti-Ago2 following p53 activation by Dox resulted in significant enrichment of miR-3189-3p but not miR-215, suggesting that miR-3189-3p is functionally involved in the p53-mediated DNA damage response (Figure 1h).

miR-3189-3p knockdown increases proliferation and sensitivity to DNA damage-induced apoptosis.

To examine the function of endogenous miR-3189-3p, we knocked down miR-3189-3p in HCT116 cells with antagomiRs (Anti-miR-3189-3p) and examined the effect on cell proliferation. Compared with mock or control (CTL) siRNA transfections, miR-3189-3p knockdown significantly increased proliferation over 4 days ($P<0.005$) (Figure 2a). In the longer term, knocking down miR-3189-3p significantly increased the clonogenicity ($P<0.0001$) of HCT116 cells (Figure 2b) seeded at a low density on plastic. These results suggested that endogenous miR-3189-3p inhibits proliferation even in the absence of genotoxic stress.

We reasoned that miR-3189-3p may play a role in the DNA damage response because of the increased incorporation of miR-3189-3p into RISC after DNA damage (Figure 1h). Therefore, we knocked down miR-3189-3p in HCT116 in combination with Dox treatment. As expected, the levels of miR-3189-3p and the p53-regulated miR-34a were elevated in CTL-transfected cells after Dox treatment, as determined by RT-qPCR (Figure 2c). miR-3189-3p was significantly down-regulated after Anti-miR-3189-3p transfection, whereas miR-34a expression remained unchanged, indicating the specificity of the miR-3189-3p antagomiR (Figure 2c). Dox treatment alone reduced the viability of CTL-transfected cells by ~1.4-fold and by greater than 3-fold in combination with silencing miR-3189-3p, suggesting that the inhibition of miR-3189-3p sensitizes cells to DNA damage (Figure 2d).

Figure 1 miR-3189 is a p53-inducible miRNA embedded in the intron of GDF15. (**a**) Genomic locus of miR-3189 and predicted miR-3189 stem-loop structure. The miR-3189 hairpin sequence begins 95 bp downstream of the 5′ splice site of *GDF15*. (**b**) Human pre-miR-3189 hairpin structure. (**c**) Multiple alignment and predicted consensus RNA secondary structure for miR-3189 candidate sequences in primates. Evolutionary analysis and phylogenetic stochastic content-free grammar models for RNA evolution give a strong prediction that the miR-3189 precursors can fold into a stable conserved miRNA-like structure in apes and old-world monkeys. The optimal conserved secondary structure in dot-bracket notation is shown. Prediction of secondary structure is based on the multiple alignment of miR-3189 precursors in primates. Profile of similarity is shown below in grey. Highly conserved base-pairs in folding are shown in red; base-pairs, formed by several combinations of nucleotides, are indicated by different colors. (**d**) Treatment of HCT116, RKO and SW48 cells with Nutlin-3 for 8 h induced *GDF15* mRNA and pri-miR-3189 expression as determined by RT-qPCR normalized to *UBC*. (**e**) *GDF15* mRNA and pri-miR-3189 are upregulated after treatment of HCT116 with 300 nM doxorubicin (Dox), as determined by RT-qPCR normalized to *GAPDH*. (**f**) A 223-nt sequence containing the miR-3189 stem-loop sequence was cloned into the expression vector pCDH. This construct was transiently transfected into HCT116 cells, and RNA was isolated after 48 h. Mature miR-3189 and miR-34a expression was assayed by TaqMan RT-qPCR. (**g**) Mature miR-3189-3p and miR-34a levels were compared between pharmacological and DNA-damage modes of p53 activation, by treatment with Nutlin-3 and Dox, respectively. Mature miRNAs were quantitated using TaqMan RT-qPCR. (**h**) Ago2 IP was conducted after 6 h of treatment with 300 nM Dox. TaqMan RT-qPCR from pulldown RNA shows significant enrichment of miR-3189-3p in RISC IP compared with IgG IP or untreated samples. The unrelated miR-215 was used as a control miRNA for the pulldowns

To investigate whether this effect is detectable in a long-term cell culture, we knocked down miR-3189-3p in HCT116 in combination with Dox treatment and then seeded the cells for colony formation assays. Consistent with our previous result (Figures 2b and d), knockdown of miR-3189-3p increased proliferation in untreated cells. The decrease in survival following DNA damage was more substantial after miR-3189-3p knockdown than with the CTL siRNA transfections (Figure 2e and Supplementary Figure S4). Interestingly, siRNA knockdown of the miR-3189 host gene GDF15 neither

promoted proliferation nor caused a reduction in steady-state levels of miR-3189-3p, indicating that miR-3189-3p has a function distinct from that of its host gene

(Supplementary Figure S5). Therefore, these results suggest that miR-3189-3p plays a role in the recovery of HCT116 cells from genotoxic stress.
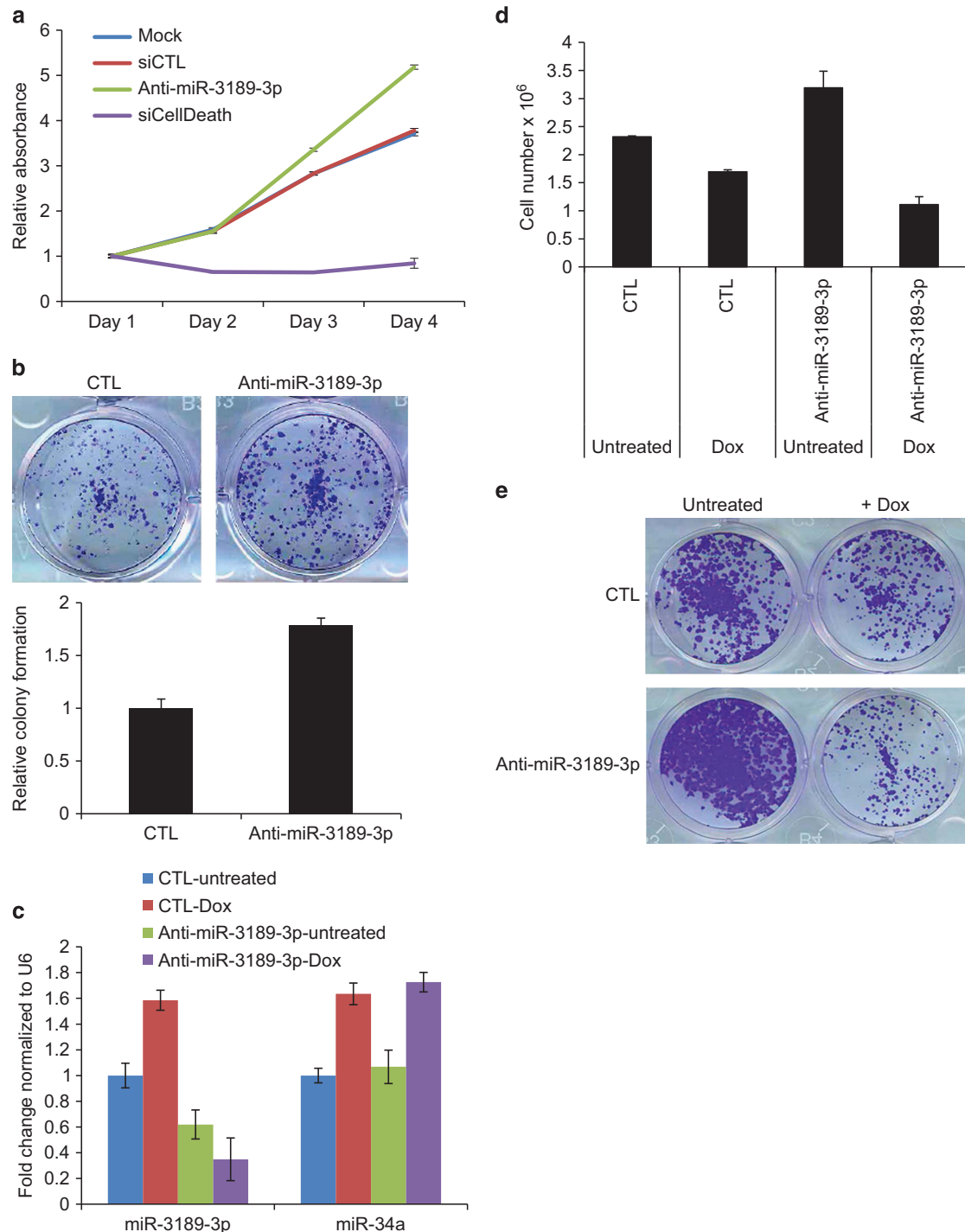
Figure 2 miR-3189 knockdown increases proliferation and sensitizes HCT116 cells to DNA damage. (**a**) miR-3189-3p inhibition promotes cell proliferation in HCT116 cells as measured by WST-8 assays. Cells were reverse-transfected with 50 nM CTL siRNA, Anti-miR-3189-3p or the positive control siCellDeath and seeded in 96-well plates. WST-8 measurements were performed over the course of 4 days (*n* = 3). (**b**) Colony formation assay performed by transfecting HCT116 cells with 50 nM Anti-miR-3189-3p and re-seeding after 48 h at a density of 1000 cells/well. Cells were fixed after 2 weeks and stained with crystal violet. (**c**) HCT116 cells were reverse-transfected with CTL siRNA or Anti-miR-3189-3p for 48 h, then treated with 300 nM Dox for 8 h. Total RNA was isolated and expression of miR-3189-3p and miR-34a was assayed by TaqMan RT-qPCR. (**d**) HCT116 cells were reverse-transfected with miR-3189-3p and treated with Dox as in (**c**). Dox was removed and cells replaced with fresh medium for a further 48 h. Live cells were counted using an automated cell counter. (**e**) HCT116 cells were reverse-transfected with CTL siRNA or Anti-miR-3189-3p and treated with Dox as in (**c**) and seeded for colony formation as in (**b**). Transfection of Anti-miR-3189-3p causes a decrease in colony formation after Dox treatment as compared with either Dox+siCTL or Untreated+Anti-miR-3189-3p

Regulation of the transcriptome by miR-3189-3p. To understand the effects of miR-3189-3p on transcriptome-wide gene expression and to begin to identify the mRNAs downregulated by miR-3189-3p, we transfected HCT116-p53WT cells with CTL or miR-3189-3p mimic and performed microarrays. Overexpression of miR-3189-3p resulted in significant downregulation (Bonferroni adjusted $P < 0.05$) of 2067 genes (Supplementary Table S1). Canonical pathways overrepresented among the downregulated genes included the mitotic roles of polo-like-kinases and cell cycle regulation (Figure 3a). We performed RT-qPCR to validate a subset of these genes also predicted by TargetScan to be direct 3'UTR targets of miR-3189-3p. We validated the downregulation of 12 out of 12 genes upon overexpression of miR-3189-3p in HCT116, which included polo-like kinase-associated genes and cell cycle regulatory genes. (Figure 3b). We next cloned the 3'UTRs of eight miR-3189-3p targets in the 3'UTR of *Renilla* luciferase of psiCHECK2 and performed luciferase reporter assays with miR-3189-3p mimics. The 3'UTRs of all genes except *CCNE2* were significantly repressed by miR-3189-3p (Figure 3c). Similarly, we observed a striking effect on the protein levels of HDAC1, HDAC3 and CDK2 upon miR-3189-3p overexpression in HCT116 cells (Figure 3d). In the context of miR-3189-3p induction by DNA damage, we would expect these target genes to be repressed. Indeed, antagonizing miR-3189-3p in the context of DNA damage derepressed CDK2 and CCNA2, and to a lesser extent CDC25A (Supplementary Figure S6A).
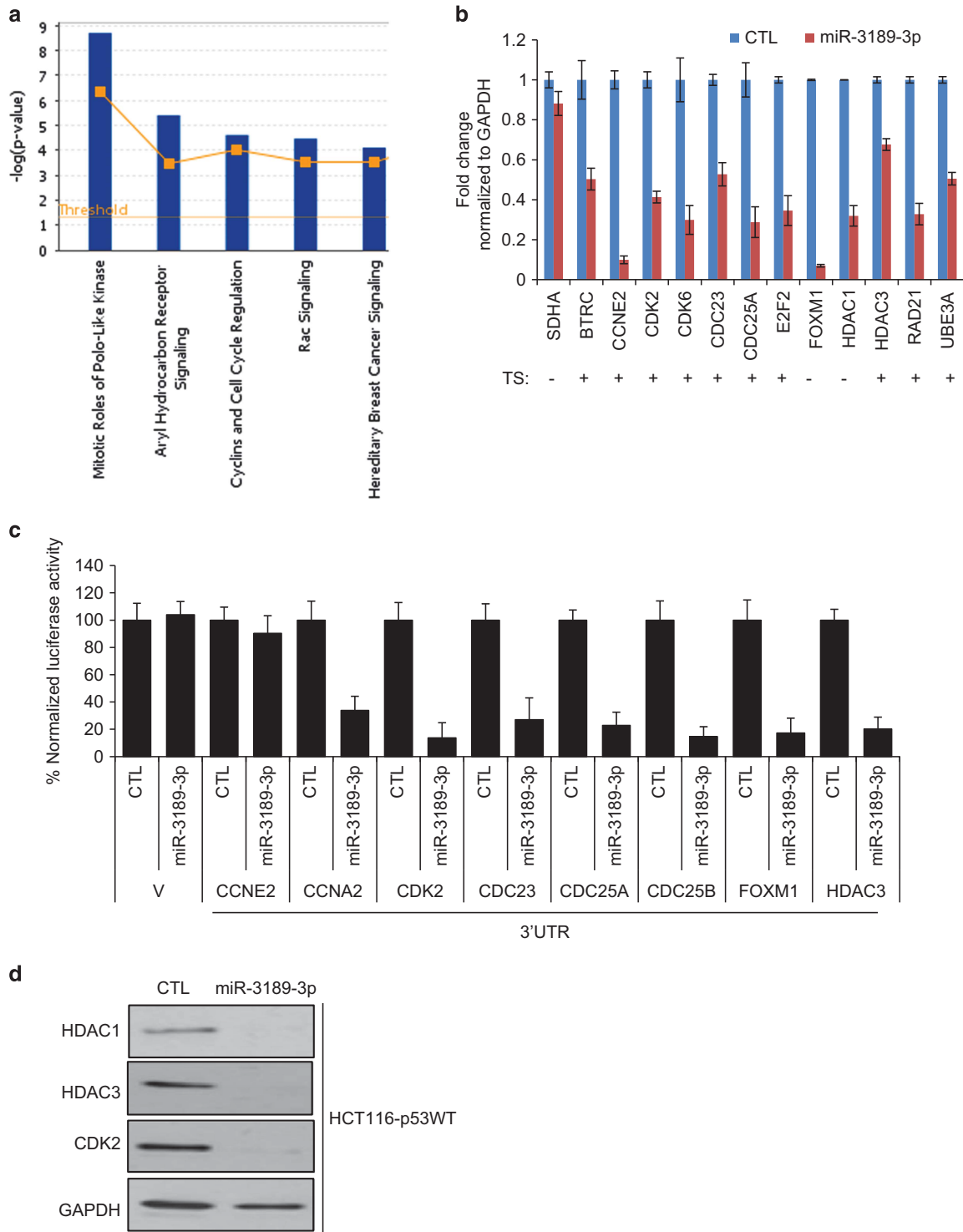
Overexpression of miR-3189-3p upregulates p53 and many p53 targets. Recent reports suggest that some p53-regulated miRNAs including miR-34a and miR-29a potentiate p53 activity by targeting inhibitors of p53.[11,17] As a result, overexpression of these miRNAs upregulates p53 target genes even in unstressed cells and induces growth arrest and apoptosis in a p53-dependent manner. Several known inhibitors of p53 such as *HDAC1, HDAC3, FOXM1, UBE3A, BCL6* and *PRKRA* were downregulated by miR-3189-3p (Supplementary Table S1). Therefore, we reasoned that miR-3189-3p may cause the upregulation of p53 and its target genes. We interrogated the HCT116 miR-3189-3p overexpression microarray data for upregulated genes using an adjusted *P*-value cutoff of $P < 0.05$. Canonical p53 pathway genes were statistically overrepresented among the 1948 genes significantly upregulated by miR-3189-3p (Figure 4a). We validated the upregulation of five p53-target genes using RT-qPCR (Figure 4b). Consistent with this result, p53 and p21 protein levels increased following miR-3189-3p overexpression in HCT116-p53WT cells (Figure 4c). Inhibition of miR-3189-3p using Anti-miRs combined with Dox treatment resulted in lesser upregulation of the p53 pathway genes *p21* and *MDM2*, supporting a role for miR-3189-3p in regulating the transcriptomic response to DNA damage (Supplementary Figure S6B).

Chromatin IP assays demonstrated increased binding of p53 to the promoters of *p21* and *GADD45A* in HCT116-p53WT cells transfected with miR-3189-3p mimics (Figure 4d). These results, in conjunction with the observed downregulation of select p53 inhibitory genes, suggest a positive feedback loop between miR-3189-3p and p53.

Provocatively, *GDF15* expression was increased almost eightfold after miR-3189-3p transfection, possibly indicating miR-3189 auto-regulation. However, this result was obtained with the use of miRNA mimics; further experiments are required to determine whether this regulatory relationship also exists between endogenous miR-3189-3p and GDF15.

Overexpression of miR-3189-3p upegulates a subset of p53 targets including *GDF15* in p53-deficient cells. Comparisons between isogenic p53 wild-type (p53WT) and p53 knockout (p53KO) cell lines have been useful in identifying p53 targets and p53-dependent effects. Therefore, we chose to use HCT116-p53KO cells as a negative control while measuring the expression of p53-target genes that were upregulated by miR-3189-3p in HCT116-p53WT cells. Although the p53-target gene *p21* was not upregulated when miR-3189-3p was overexpressed in HCT116-p53KO, we were surprised to see the upregulation of select p53 targets including *GADD45A* and *GDF15* in HCT116-p53KO cells (Figure 4e). In order to ascertain the full extent of these p53-independent effects of miR-3189-3p, we performed micro-arrays from HCT116-p53KO cells following miR-3189-3p mimic transfection (Supplementary Table S2). Consistent with our RT-qPCR results (Figure 4e), we observed increased levels of *GADD45A* and *GDF15* mRNAs. Interestingly, we also found significant upregulation of the p53 targets *NOXA, p53R2, RCHY1* and *SCOTIN,* which we validated by RT-qPCR (Figure 4e). Although comparatively fewer genes were significantly downregulated in HCT116-p53KO cells than in p53WT, 82% of the genes downregulated in HCT116-p53KO cells were also significantly reduced in HCT116-p53WT cells ($P < 10^{-30}$) (Figure 4f). We performed RT-qPCR to further validate decreased expression of a subset of these genes that play important roles in cell proliferation including *CDK6* and *E2F1* (Figure 4g). Downregulation of *HDAC1, HDAC3* and *CDK2* protein was also validated (Figure 4h). Collectively, these results not only identified several key cell cycle progression genes as miR-3189-3p targets in both p53WT and p53KO cells but also indicated the existence of a yet unknown mechanism by which a subset of canonical p53 targets were upregulated in the absence of p53.

miR-3189-3p kills cells irrespective of p53 status. To examine the phenotypic effects of miR-3189 overexpression, we began by transiently overexpressing miR-3189-3p and -5p mimics into isogenic HCT116-p53WT and HCT116-p53KO cells. We included miR-3189-5p to determine whether the minor product of the miR-3189 stem-loop has some functional significance. We found that miR-3189-3p, but not miR-3189-5p, potently inhibited viability of both cell lines (Figure 5a). Strikingly, in HCT116 cells, miR-3189-3p mimics were almost as toxic as siCellDeath (Figure 5b). Because the effect on cell viability was so profound, we wondered whether supraphysiological levels of miRNA mimic cause off-target toxicity. However, when we measured the amount of exogenous miRNA incorporated into RISC, we found it to be within physiological levels (Supplementary Figure S7), consistent with what we and others have recently reported for other miRNAs.[27–29] Combination with GDF15 siRNA significantly reduced the effect of miR-3189-3p mimic,

Figure 3 Overexpression of miR-3189-3p downregulates multiple cell cycle genes. (**a**) HCT116 cells were reverse-transfected with CTL or miR-3189-3p mimic for 48 h and microarrays were performed. Genes downregulated by miR-3189-3p mimic (adjusted $P < 0.05$) were interrogated by Ingenuity canonical pathway analysis. (**b**) Select genes identified as significantly downregulated in the microarrays were validated using RT-qPCR, normalized to *GAPDH*. Presence or absence of predicted miR-3189-3p binding sites (TargetScan) in the 3'UTR are indicated with TS+ or -, respectively. (**c**) Reporter constructs containing full length 3'UTRs of selected miR-3189-3p target genes or empty vector (V) were co-transfected with miR-3189-3p mimic into HCT116 cells. Luciferase assays were performed after 48 h and presented as average percent luciferase activity +/− S.E.M. ($n = 3$). (**d**) Protein levels of miR-3189-3p targets HDAC1, HDAC3 and CDK2 were assessed by immunoblotting 48 h after transfection of HCT116 cells with CTL or miR-3189-3p mimic
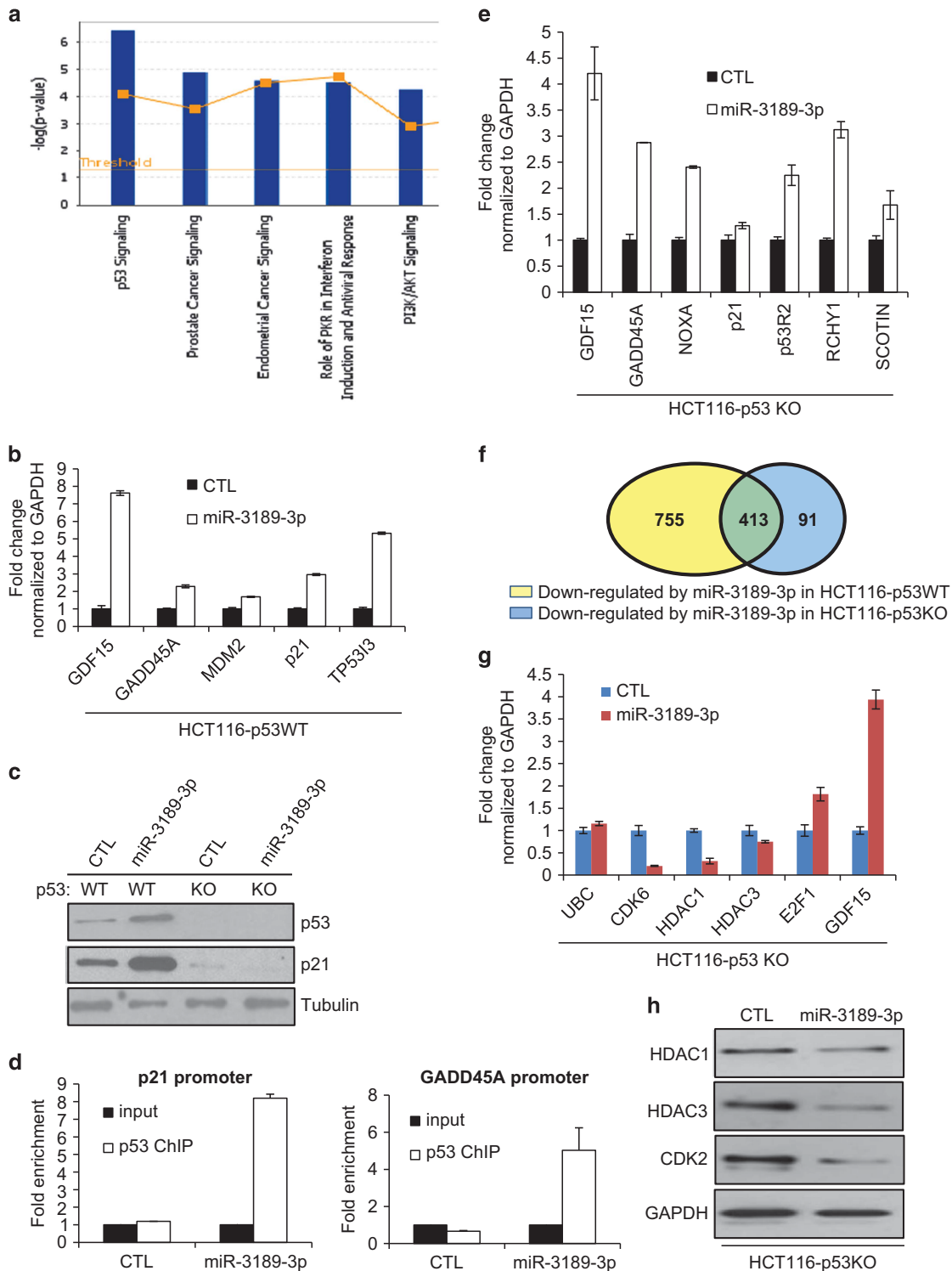
Figure 4 Overexpression of miR-3189-3p activates the p53 pathway. (**a**) The set of genes upregulated in the miR-3189-3p microarrays with an adjusted *P*-value < 0.05 were subjected to Ingenuity canonical pathway analysis. (**b**) The mRNA expression of five canonical p53 target genes was assayed 48 h after miR-3189-3p mimic transfection in HCT116-p53WT by RT-qPCR, normalized to *GAPDH*. (**c**) Upregulation of p53 and p21 proteins following miR-3189-3p mimic transfection into HCT116-p53WT was confirmed by immunoblotting. Tubulin was used as loading control. (**d**) Recruitment of p53 protein to the promoters of its canonical targets *p21* and *GADD45A* 48 h after miR-3189-3p mimic transfection in HCT116-p53WT was assayed by ChIP-qPCR. Both promoters were enriched in p53-ChIP samples compared with *GAPDH* promoter following miR-3189-3p transfection. (**e**) mRNA expression of p53 target genes was assayed by RT-qPCR in HCT116-p53KO cells 48 h after miR-3189-3p mimic transfection, normalized to *GAPDH*. (**f**) RNA was isolated from HCT116p53-KO cells transfected for 48 h with either CTL or miR-3189-3p mimic and subjected to microarrays. A total of 504 transcripts were significantly downregulated (adjusted $P < 0.05$) in HCT116-p53KO, of which 413 were also downregulated in HCT116-p53WT ($P < 10^{-30}$, as determined using a normal approximation of the exact hypergeometric probability). (**g**, **h**) Select genes in the intersection of downregulated genes in HCT116-p53WT and -KO microarrays were validated at the mRNA and protein levels by RT-qPCR and immunoblotting, respectively
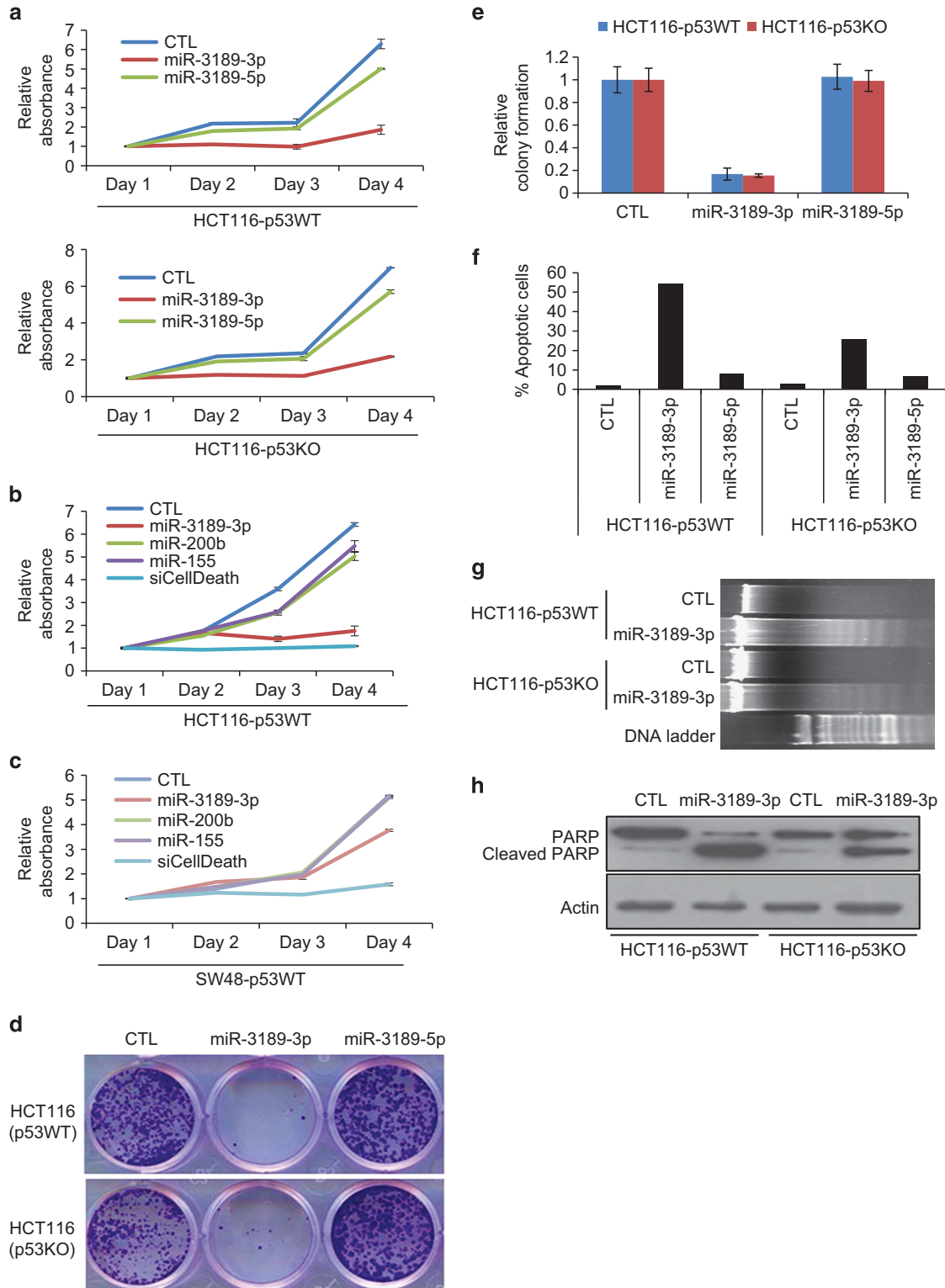
Figure 5 miR-3189-3p induces apoptosis independently of p53 status. (**a**) HCT116-p53WT or -KO cells were reverse-transfected with CTL siRNA, miR-3189-3p or -5p mimics and seeded in 96-well plates for WST-8 assays. WST-8 assays were performed over a period of 4 days. (**b, c**) The effect of miR-3189-3p in HCT116-p53WT and SW48-p53WT cells was compared with the controls siCellDeath, miR-155 and miR-200b. Assays were conducted as described in (**a**). (**d, e**) HCT116-p53WT and -KO cells were reverse-transfected for 48 h, then trypsinized and re-seeded and allowed to grow for 2 weeks. Colonies were fixed in methanol and stained with crystal violet. (**f**) HCT116-p53WT or -KO cells were reverse-transfected with miR-3189-3p mimic and fixed after 48 h. DNA content was measured by propidium iodide staining and FACS analysis. Cells with DNA content less than 2 N (sub-G1 apoptotic) are shown as a percentage of total cells. (**g**) DNA was isolated from HCT116-WT or -p53KO cells 48 h after reverse transfection with CTL or miR-3189-3p mimics, and DNA fragmentation was assayed by agarose gel electrophoresis. (**h**) Whole-cell lysates from HCT116-WT and -p53KO were prepared 48 h after transfection with CTL siRNA or miR-3189-3p mimic and immunoblotted for poly-ADP ribose polymerase (PARP) and actin (loading control)

suggesting that the positive feedback interaction between miR-3189-3p and its host gene is important for miR-3189-3p function (Supplementary Figure S5C).

Importantly, the lethal effects of miR-3189-3p were not restricted to HCT116 cells. Similar potency was observed in the mutant p53 MDA-MB-231 cells (Supplementary Figure S8). However, the effect of miR-3189-3p was less pronounced in SW48 cells (Figure 5c). Despite the apoptotic effect of miR-3189-3p in cancer cells, it is expressed in several normal human tissues, particularly colon, prostate and placenta (Supplementary Figure S9A). To test whether miR-3189-3p was specifically lethal to cancer cells, we transfected miR-3189-3p mimics into the normal-like WI38 and MCF10A cells and observed less cell death as compared with HCT116 and MDA-MB-231 cells (Supplementary Figure S9B).

Consistent with its growth inhibitory effects, overexpression of miR-3189-3p, but not miR-3189-5p, resulted in a dramatic reduction in colony formation on plastic after 10 days in isogenic p53WT- and p53KO-HCT116 cells (Figures 5d and e). To determine whether the effect of miR-3189-3p was due to growth arrest or induction of apoptosis, we transfected the isogenic HCT116 lines with CTL, miR-3189-3p or -5p mimics for 48 h and stained cells with propidium iodide. miR-3189-3p, but not CTL or miR-3189-5p, induced a sub-G1 shoulder in ~55% of HCT116-p53WT cells and ~25% of HCT116-p53KO cells, suggesting that miR-3189-3p induces apoptosis (Figure 5f). Moreover, HCT116-p53WT and HCT116-p53KO cells transfected with miR-3189-3p mimic also displayed increased levels of DNA fragmentation (Figure 5g) and PARP cleavage (Figure 5h). Overexpression of miR-3189-3p into HCT116-p53WT cells also resulted in upregulation of the p53-associated mediators of apoptosis PUMA and BAX at the protein level (Supplementary Figure S10), further confirming that miR-3189-3p mimics induce apoptosis. In order to determine whether this apoptotic effect was dosage-dependent, with lower concentrations of mimic favoring cell cycle arrest over apoptosis, we titrated miR-3189-3p mimic concentrations followed by propidium iodide staining. Lower concentrations of miR-3189-3p mimic (5 and 10 nM) also mediated repression of miR-3189-3p target genes and caused cell death (Supplementary Figure S11A, and S11B). At 1 nM, miR-3189-3p targets were not downregulated and neither apoptosis nor cell cycle arrest was observed. Because the positive control siCellDeath was effective at 1 nM (Supplementary Figure S11C), we conclude that the transfection efficiency does not limit the efficacy of miR-3189 at low concentrations, but rather the amount of miRNA mimic introduced into transfected cells at 1 nM is too low to repress gene expression.

miR-3189-3p inhibits colony formation *in vitro* and tumorigenesis *in vivo*. In addition to its effects on cell proliferation on plastic, we observed that in HCT116-p53WT and isogenic p53KO cells, miR-3189-3p mimics inhibited anchorage-independent growth on soft agar (Figure 6a). Because soft agar colony formation approximates tumorigenic potential, we hypothesized that miR-3189-3p also inhibits tumorigenicity in xenograft models. Therefore, we subcutaneously injected NOD-SCID mice with HCT116-p53WT or HCT116-p53KO cells transfected with CTL or

miR-3189-3p mimic. miR-3189-3p overexpression dramatically reduced the rate of xenograft growth over 4 weeks in both cell lines (Figure 6b). The average tumor volume after 4 weeks was ~ 2000-fold greater in mice injected with either of the CTL-transfected lines than in mice injected with miR-3189-3p-transfected cells (Figure 6c and d). Together, the results from this study suggest that miR-3189-3p is a novel p53-regulated miRNA that plays a role in cell survival during the DNA damage response, whereas introduction of exogenous miR-3189-3p strongly induces apoptosis even in cells lacking wild-type p53.

Discussion

In this study, we have combined gene expression profiling in the context of p53 activation with functional experiments to characterize the biogenesis and functions of a novel, primate-specific miRNA: miR-3189. Previous RNA-seq studies indicated the existence of a mature miRNA that maps to the intron of *GDF15*. Our work represents the first validation and functional study of miR-3189. We have shown that the 3p product of the miR-3189 stem loop is a *bona fide* miRNA, which is more abundant than miR-3189-5p, preferentially incorporated into RISC and required for cell viability following DNA damage.

Many miRNAs are produced from loci within introns of protein-coding genes or spliced non-coding transcripts.[1,30,31] Although these intronic miRNAs may be regulated independently of their host genes by discrete promoters,[27,32] there are also instances in which an embedded miRNA and its host gene are transcriptionally co-regulated.[33] *GDF15* and miR-3189 have similar expression patterns across panels of both healthy tissues and colorectal cancer patient samples (TCGA, data not shown). Our results indicate that *GDF15* and miR-3189-3p are transcriptionally co-regulated by p53. This conclusion is further supported by a recent study in which global run-on sequencing was used to profile nascent transcripts shortly after p53 activation. In that study, GDF15 and miR-3189 were observed to be rapidly upregulated following Nutlin-3 treatment.[34]

Studies on the roles of *GDF15* (also known as *MIC1* or *NAG1*) have produced conflicting reports, and it has been implicated in a wide range of cellular processes.[35] *GDF15* has been reported by multiple studies to be a target of p53 in response to both DNA damage and p53 induction by Nutlin-3,[4–6,20,36,37] and these and other results have attributed growth-inhibitory and tumor-suppressive functions to *GDF15*.[7–11,38,39] However, other studies have found elevated expression of *GDF15* in many human cancers,[15,40–42] and high levels of *GDF15* expression correspond to increased metastasis in both mouse models and human patients.[16–20,41,43] Although it is possible that *GDF15* exerts pleiotropic effects on the growth of cancer cells, prior studies may have conflated the function of GDF15 with that of the embedded miR-3189. For example, p53-independent upregulation of *GDF15* by the long non-coding RNA MEG3 causes growth arrest in HCT116-p53KO cells,[21,44] which conflicts with earlier reports regarding GDF15 function,[22–24,45,46] yet is completely consistent with our results showing the p53-independent effects of miR-3189-3p. We have shown that the knockdown of GDF15 has a growth inhibitory
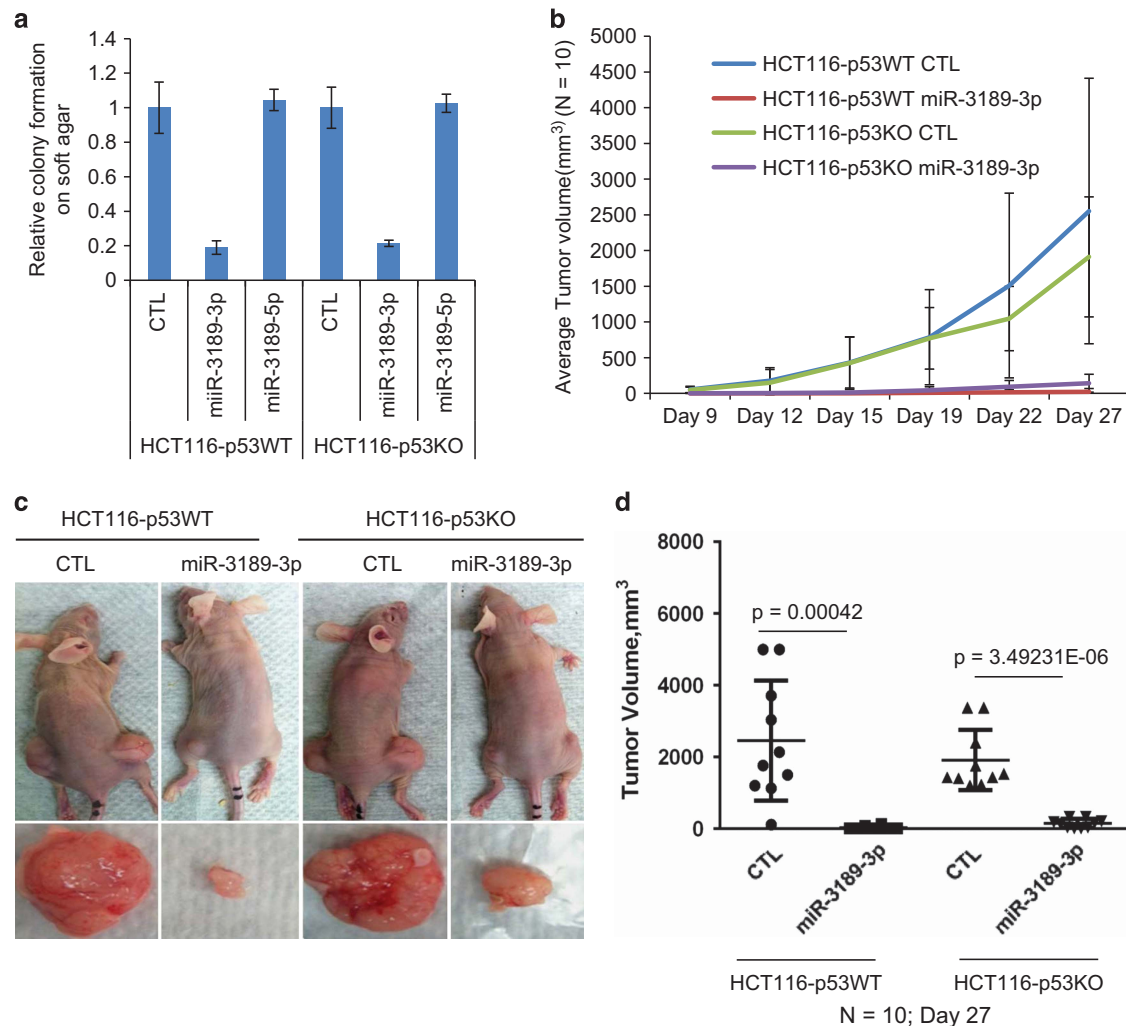
Figure 6 miR-3189 suppresses tumorigenicity *in vitro* and *in vivo*. (**a**) HCT116-p53WT or -p53KO cells were reverse-transfected with CTL siRNA, miR-3189-3p or -5p mimics and seeded in soft agar after 48 h. The transfectants were grown in soft agar for 3 weeks and colonies were counted under a light microscope. Data presented ± S.E.M., *n* = 3. (**b**–**d**) HCT116-WT or -p53KO transfected for 36 h with CTL siRNA or miR-3189-3p mimic were injected subcutaneously into the flanks of athymic nude mice (*n* = 10). Mice were killed after 27 days. (**b**) Tumor volume in mice from was measured by caliper assessment over 16 days starting 9 days after injection. (**c**) Mice were killed after 4 weeks, tumors were excised and weighed. (**d**) Average tumor mass from mice injected with transfected *versus* untransfected cells compared using two-tailed student's *t*-test

effect, whereas antagonizing miR-3189-3p causes an increase in proliferation, which highlights the importance of distinguishing the effects of miR-3189 from those of its host gene. However, we have also shown that miR-3189-3p expression results in increased GDF15 transcription, and this feedback loop seems to be important for the downstream effects of miR-3189-3p. Our study has established miR-3189-3p as integral to the cellular response to genotoxic stress, and miR-3189-3p may also be involved in the response to hypoxia or inflammatory stress, which have also been shown to upregulate GDF15.[25,45,13,17,46,44]

Our results have identified miR-3189-3p as a miRNA that can kill cancer cells independently of p53. miR-34a, the most extensively studied p53-regulated miRNA, is involved in positive feedback loops with p53 by repressing the p53 inhibitors SIRT1[47] and HDM4,[11] but several studies suggest that its effects, unlike those of miR-3189-3p, depend on the presence of wild-type p53.[11,12,48] Our results indicate that

miR-3189-3p also mediates a positive feedback loop in which p53 activation is sustained by downregulation of the known p53 inhibitors HDAC1 and HDAC3.[33,49,50] We found that miR-3189-3p knockdown increases cell death following DNA damage. This effect is consistent with a putative role in the DNA damage response: without miR-3189-3p, cells are ill-equipped to recover from genotoxic stress. Re-introduction of miR-3189-3p into p53-null cancer cell lines caused strong apoptotic responses and upregulation of a subset of p53 target genes including *GADD45A* and *GDF15*. However, the increase in proliferation caused by miR-3189-3p inhibition may also indirectly sensitize cells to DNA damage.

Because p53 is the most frequently mutated gene in human cancers, a miRNA that circumvents mutant p53 to induce apoptosis offers significant promise for cancer therapy. Over the past 5 years, much research has focused on developing methods to target oncogenic miRNAs and restore tumor-suppressive miRNAs for cancer therapy.[35,51,52] The

efficacy of any new cancer therapy must be rigorously tested in animal models, most commonly murine, before it can be applied to human patients. This presents a problem: how can a primate-specific miRNA be tested in a non-primate model? Although our results demonstrate that pre-treatment of cancer cells with synthetic miR-3189-3p greatly reduces xenograft tumor growth, further *in vivo* work using xenotransplantation of human tissue may facilitate validation of miR-3189-3p as a potential therapeutic molecule, but it remains to be seen whether miR-3189-3p would have an effect on transgenic mouse models of autochthonous tumor growth or whether systemic delivery of miR-3189-3p mimic would specifically and effectively target preformed tumors. However, miR-3189-3p overexpression represents an attractive tool to either kill cancer cells by directly introducing a miRNA mimic or to sensitize cells to genotoxic chemotherapy by miR-3189-3p inhibition.

Materials and Methods

Cell culture, miRNA reagents and transfections. The colorectal cancer cell lines HCT116-p53WT and HCT116-p53KO were kindly provided by Dr. Bert Vogelstein (Johns Hopkins University, Baltimore, MD, USA). SW48, RKO, MCF10A and MDA-MB-231 cells were purchased from ATCC (Manassas, VA, USA). All cell lines were maintained in Dulbecco's modified Eagle's medium supplemented with 10% fetal bovine serum and 1% penicillin-streptomycin at 37 °C, 5% CO_2.

All miRNA mimics were purchased from Dharmacon/Thermo scientific (Pittsburg, CA, USA). The Allstars Negative (CTL) and siCellDeath siRNAs were purchased from Qiagen (Valencia, CA, USA). All miRNA mimics and siRNA transfections were performed by reverse transfection at a final concentration of 20 nM (except Supplementary Figure S10) using Lipofectamine RNAiMAX (Life technologies, Grand Island, NE, USA) as directed by the manufacturer. Anti-miR-3189-3p was purchased from Ambion (Grand Island, NE, USA) and used at a final concentration of 50 nM. Primary miR-3189 including the stemloop was PCR-amplified from genomic DNA and cloned into pCDH lentiviral vector.

Luciferase reporter assays. The 3'UTRs of miR-3189-3p target genes (Figure 3b) were amplified by PCR (primer sequences in Supplementary Table S3) from HCT116 cDNA and inserted into the *Renilla* luciferase 3'UTR of psiCHECK2 (Promega, Madison, WI, USA). Reporter assays were performed in HCT116 cells using the dual-luciferase reporter system (Promega).

RNA isolation, RT-qPCR and miRNA analysis. Total RNA was isolated using TRIzol reagent (Invitrogen, Grand Island, NE, USA) as directed by the manufacturer. Normal tissue RNA was purchased from Clontech (Mountain View, CA, USA). For RT-qPCR analysis, 500 ng total RNA was reverse-transcribed using iScript Reverse Transcription kit (Bio-Rad, Hercules, CA, USA), and qPCR was performed by using Fast SYBR Green Master Mix (Life technologies) per the manufacturer's instructions. Primer sequences are detailed in Supplementary Table S3. TaqMan miRNA assays (Life Technologies) were used to quantitate mature miRNAs following the manufacturer's instructions. *U6* snRNA was used as an internal control.

Small RNA sequencing. Total RNA was size-fractionated by denaturing PAGE, from which RNAs of 18–30nt in length were purified. The small RNA fraction was ligated to Illumina sequencing adapters and used as a template for the creation of cDNA library. Libraries were sequenced on an Illumina Genome Analyzer II platform (Illumina, San Diego, CA, USA). Illumina smRNA sequencing adapters were removed from the sequence data prior to alignment to the Hg19 reference genome using BWA. Expression levels were estimated from the aligned data by counting the number of read-tags overlapping the genomic location of mature miRNA loci, separately for matches to the positive and negative strands. Read counts were normalized by dividing counts by the average of the read count for mature miRNA in the 2nd and 3rd quartile of strand-selected reads.

Immunoblotting. Whole-cell lysates were prepared using radioimmunoprecipitation buffer containing protease inhibitor cocktail (Roche, Nutley, NJ, USA). Proteins were quantified using the bicinchoninic acid protein quantitation kit (Thermo Scientific, Waltham, MA, USA). Ten micrograms of whole-cell lysate per lane was used for immunoblotting. The following antibodies were used: DO1 anti-p53, and C19 anti-p21 (Santa Cruz, Dallas, TX, USA) at 1 : 5000 dilution; D2ELL anti-BAX, BF683 anti-CCNA2, 3652 anti-CDC25A,10E2 anti-HDAC1, 7G6C5 anti-HDAC3, 78B2 anti-CDK2, D30C10 anti-PUMA, 9F3 anti-Tubulin and 14C10 anti-GAPDH (Cell Signaling, Danvers, MA, USA), at 1 : 1000 dilution.

Cell proliferation and colony formation assays. Cell proliferation assays were performed after transfecting CTL or miRNA mimics and seeding 1500 cells per well of a 96-well plate. Cell viability was measured with the Cell Counting Kit-8, which uses the reduction of the tetrazolium salt WST-8 by live cells to assay relative proliferation (Dojindo, Rockville, MD, USA). For colony formation on plastic, cells were reverse-transfected with a CTL siRNA or miRNA mimics for 48 h, trypsinized and 1000 cells were seeded per well of 6-well plate. After 2 weeks, cells were fixed with methanol for 5 min, stained with crystal violet, and colonies were counted. For soft agar colony formation assays, cells were transfected with CTL siRNA or miRNA mimic for 48 h, trypsinized, seeded in soft agar at 1000 cells/well in a 12-well plate. Colonies were counted after 3 weeks.

Flow cytometry assays. Cells were transfected with a CTL siRNA or miRNA mimics for 72 h, fixed with ice-cold ethanol for 24 h and stained with propidium iodide (Sigma, St Louis, MO, USA) in the presence of RNase A. DNA content was analyzed on a FACSCalibur flow cytometer (BD Biosciences, San Jose, CA, USA); data were analyzed using FlowJo software.

Xenograft assays. Animal protocols were approved by the National Cancer Institute Animal Care and Use Committee following AALAAC guidelines and policies. HCT116-p53WT and HCT116-p53KO cells were transfected with CTL or miR-3189-3p mimic for 36 h, then trypsinized and washed with PBS. Live cells were counted with trypan blue exclusion and equal numbers of live cells were injected for each sample. Cells (1×10^6) were mixed with 30% matrigel in PBS on ice and the mixture was injected into the flanks of 6–8-week-old female athymic nude mice (Animal Production Program, Frederick, MD, USA) (each group $N = 10$). Tumor volume was measured twice weekly after 2 weeks of injection.

Microarray analysis. HCT116-p53WT and HCT116-p53KO cells were reverse-transfected with CTL or miR-3189-3p mimics; 48 h later, total RNA was isolated using the RNeasy Mini kit (Qiagen). Samples for microarray were labeled using the IlluminaTotalPrep RNA amplification kit (Ambion). Microarrays were performed with the HumanHT-12 v4 Expression BeadChip kit (Illumina) and analyzed in the R/Bioconductor package (Bioconductor, Seattle, WA, USA). Microarray data have been deposited to Gene Expression Omnibus (GSE62467).

Chromatin IP assays. Chromatin IP was performed with the Active Motif ChIP kit (Active Motif, Carlsbad, CA, USA) as directed by the manufacturer. Briefly, HCT116 cells were grown in 10 cm plates. Chromatin was cross-linked with 1% formaldehyde, and cells were lysed and sonicated. Protein–DNA complexes were immunoprecipitated with control IgG or anti-p53 (DO1) antibody (Santa Cruz). The IP material was washed and heated at 65 °C overnight to reverse crosslinks. Chromatin IP DNA was column purified (Qiagen), and qPCR was performed by using primers flanking the p53 binding sites in the *p21* and *GADD45A* promoters (Supplementary Table S3).

IP of Ago2-associated miRNAs. Cytoplasmic extracts were prepared from HCT116 cells as described previously.[53] Ago2 was IPed from cytoplasmic extracts using a monoclonal Ago2 antibody, a kind gift from Dr Zissimos Mourelatos (University of Pennsylvania, USA). HCT116 cells were transfected with miRNA mimics for 48 h, and cytoplasmic extracts treated with protease inhibitor (Roche) and RNaseOUT (Invitrogen) were used for IP. Ago2-miRNA complexes were subjected to IP with IgG or Ago2 antibody for 4 h at 4 °C. Antibody–ribonucleoprotein complexes were IPed with protein-G sepharose beads (Roche). RNA was isolated by phenol-chloroform extraction (Ambion) followed by ethanol precipitation and TaqMan RT-qPCR.

Comparative genome analysis. Multiple alignments of mammalian orthologous regions for human miR-3189 precursor were created using the Muscle

sequence alignment software.[54] miR-3189 candidates were mapped to mammalian genomes using BLAST[55] or LiftOver.[56] On the basis of the reciprocal BLAST hits and analysis of syntenic regions, we identified 14 orthologous candidates for miR-3189 precursors in different mammalian genomes. Phylogenetic analysis was conducted using MEGA5 and RAxML software.[57,58] RNA secondary structures for single sequences and for multiple alignments were predicted by Afold and Alifold respectively.[59,60]

Conflict of Interest

The authors declare no conflict of interest.

1. Wightman B, Ha I, Ruvkun G. Posttranscriptional regulation of the heterochronic gene lin-14 by lin-4 mediates temporal pattern formation in C. elegans. *Cell* 1993; **75**: 855–862.
2. Lee RC, Feinbaum RL, Ambros V. The C. elegans heterochronic gene lin-4 encodes small RNAs with antisense complementarity to lin-14. *Cell* 1993; **75**: 843–854.
3. Ameres SL, Zamore PD. Diversifying microRNA sequence and function. *Nat Rev Mol Cell Biol* 2013; **14**: 475–488.
4. Esteller M. Non-coding RNAs in human disease. *Nat Rev Genet* 2011; **12**: 861–874.
5. Lujambio A, Lowe SW. The microcosmos of cancer. *Nature* 2012; **482**: 347–355.
6. Kumar MS, Pester RE, Chen CY, Lane K, Chin C, Lu J et al. Dicer1 functions as a haploinsufficient tumor suppressor. *Genes Dev* 2009; **23**: 2700–2704.
7. Jones M, Lal A. MicroRNAs, wild-type and mutant p53: more questions than answers. *RNA Biol* 2012; **9**: 781–791.
8. Hermeking H. MicroRNAs in the p53 network: micromanagement of tumour suppression. *Nat Rev Cancer* 2012; **12**: 613–626.
9. Leung AKL, Sharp PA. MicroRNA functions in stress responses. *Mol Cell* 2010; **40**: 205–215.
10. Raver-Shapira N, Marciano E, Meiri E, Spector Y, Rosenfeld N, Moskovits N et al. Transcriptional activation of miR-34a contributes to p53-mediated apoptosis. *Mol Cell* 2007; **26**: 731–743.
11. Okada N, Lin C-P, Ribeiro MC, Biton A, Lai G, He X et al. A positive feedback between p53 and miR-34 miRNAs mediates tumor suppression. *Genes Dev* 2014; **28**: 438–450.
12. Chang T-C, Wentzel EA, Kent OA, Ramachandran K, Mullendore M, Lee KH et al. Transactivation of miR-34a by p53 broadly influences gene expression and promotes apoptosis. *Mol Cell* 2007; **26**: 745–752.
13. Lal A, Thomas MP, Altschuler G, Navarro F, O'Day E, Li XL et al. Capture of microRNA-bound mRNAs identifies the tumor suppressor miR-34a as a regulator of growth factor signaling. *PLoS Genet* 2011; **7**: e1002363.
14. Navarro F, Gutman D, Meire E, Caceres M, Rigoutsos I, Bentwich Z et al. miR-34a contributes to megakaryocytic differentiation of K562 cells independently of p53. *Blood* 2009; **114**: 2181–2192.
15. Bohlig L, Friedrich M, Engeland K. p53 activates the PANK1/miRNA-107 gene leading to downregulation of CDK6 and p130 cell cycle proteins. *Nucleic Acids Res* 2011; **39**: 440–453.
16. Huarte M, Guttman M, Feldser D, Garber M, Koziol MJ, Kenzelmann-Broz D et al. A large intergenic noncoding RNA induced by p53 mediates global gene repression in the p53 response. *Cell* 2010; **142**: 409–419.
17. Park S-Y, Lee JH, Ha M, Nam J-W, Kim VN. miR-29 miRNAs activate p53 by targeting p85 alpha and CDC42. nature structural &. *Mol Biol* 2009; **16**: 23–29.
18. Persson H, Kvist A, Rego N, Staaf J, Vallon-Christersson J, Luts L et al. Identification of new microRNAs in paired normal and tumor breast tissue suggests a dual role for the ERBB2/Her2 gene. *Cancer Res* 2011; **71**: 78–86.
19. Stark MS, Tyagi S, Nancarrow DJ, Boyle GM, Cook AL, Whiteman DC et al. Characterization of the melanoma miRNAome by deep sequencing. *PLoS ONE* 2010; **5**: e9685.
20. Cheng J-C, Chang H-M, Leung PCK. Wild-type p53 attenuates cancer cell motility by inducing growth differentiation factor-15 expression. *Endocrinology* 2011; **152**: 2987–2995.
21. Bootcov MR, Bauskin AR, Valenzuela SM, Moore AG, Bansal M, He XY et al. MIC-1, a novel macrophage inhibitory cytokine, is a divergent member of the TGF-beta superfamily. *Proc Natl Acad Sci USA* 1997; **94**: 11514–11519.
22. Friedman RC, Farh KKH, Burge CB, Bartel DP. Most mammalian mRNAs are conserved targets of microRNAs. *Genome Res* 2008; **19**: 92–105.
23. Perdomo C, Campbell JD, Gerrein J, Tellez CS, Garrison CB, Walser TC et al. MicroRNA 4423 is a primate-specific regulator of airway epithelial cell differentiation and lung carcinogenesis. *Proc Natl Acad Sci USA* 2013; **110**: 18946–18951.
24. Piriyapongsa J, Jordan IK. A family of human microRNA genes from miniature inverted-repeat transposable elements. *PLoS One* 2007; **2**: e203.
25. Hu B, Ying X, Wang J, Piriyapongsa J, Jordan IK, Sheng J et al. Identification of a tumor suppressive humanspecific microRNA within the FHIT tumor suppressor gene. *Cancer Res* 2014; **74**: 2283–94.
26. Arcila ML, Betizeau M, Cambronne XA, Guzman E, Doerflinger N, Bouhallier F et al. Novel primate miRNAs coevolved with ancient target genes in germinal zone-specific expression patterns. *Neuron* 2014; **81**: 1255–1262.
27. Subramanian M, Francis P, Bilke S, Li XL, Hara T, Lu X et al. A mutant p53/let-7i-axis-regulated gene network drives cell migration, invasion and metastasis. *Oncogene* e-pub ahead of print 24 March 2014.
28. Li XL, Hara T, Choi Y, Subramanian M, Francis P, Bilke S et al. A p21-ZEB1 complex inhibits epithelial-mesenchymal transition through the microRNA 183-96-182 cluster. *Mol Cell Biol* 2014; **34**: 533–550.
29. Thomson DW, Bracken CP, Szubert JM, Goodall GJ. On measuring miRNAs after transient transfection of mimics or antisense inhibitors. *PLoS ONE* 2013; **8**: e55214.
30. Kim VN, Han J, Siomi MC. Biogenesis of small RNAs in animals. *Nat Rev Mol Cell Biol* 2009; **10**: 126–139.
31. Rearick D, Prakash A, McSweeny A, Shepard SS, Fedorova L, Fedorov A. Critical association of ncRNA with introns. *Nucleic Acids Res* 2011; **39**: 2357–2366.
32. Monteys AM, Spengler RM, Wan J, Tecedor L, Lennox KA, Xing Y et al. Structure and activity of putative intronic miRNA promoters. *RNA* 2010; **16**: 495–505.
33. Xiao J, Lin H, Luo X, Luo X, Wang Z. miR-605 joins p53 network to form a p53:miR-605:Mdm2 positive feedback loop in response to stress. *EMBO J* 2011; **30**: 524–532.
34. Allen MA, Andrysik Z, Dengler VL, Mellert HS, Guarnieri A, Freeman JA et al. Global analysis of p53-regulated transcription identifies its direct targets and unexpected regulatory mechanisms. *Elife* 2014; **3**: e02200.
35. Mimeault M, Batra SK. Divergent molecular mechanisms underlying the pleiotropic functions of macrophage inhibitory cytokine-1 in cancer. *J Cell Physiol* 2010; **224**: 626–635.
36. Djuranovic S, Nahvi A, Green R. A Parsimonious Model for Gene Regulation by miRNAs. *Science* 2011; **331**: 550–553.
37. Li PX, Wong J, Ayed A, Ngo D, Brade AM, Arrowsmith C et al. Placental transforming growth factor-beta is a downstream mediator of the growth arrest and apoptotic response of tumor cells to DNA damage and p53 overexpression. *J Biol Chem* 2000; **275**: 20127–20135.
38. Kelly JA, Lucia MS, Lambert JR. p53 controls prostate-derived factor/macrophage inhibitory cytokine/NSAID-activated gene expression in response to cell density, DNA damage and hypoxia through diverse mechanisms. *Cancer Lett* 2009; **277**: 38–47.
39. Yang H, Filipovic Z, Brown D, Breit SN, Vassilev LT. Macrophage inhibitory cytokine-1: a novel biomarker for p53 pathway activation. *Mol Cancer Ther* 2003; **2**: 1023–1029.
40. Brown DA, Ward RL, Buckhaults P, Liu T, Romans KE, Hawkins NJ et al. MIC-1 serum level and genotype: associations with progress and prognosis of colorectal carcinoma. *Clin Cancer Res* 2003; **9**: 2642–2650.
41. Xue H, Lü B, Zhang J, Wu M, Huang Q, Wu Q et al. Identification of serum biomarkers for colorectal cancer metastasis using a differential secretome approach. *J Proteome Res* 2010; **9**: 545–555.
42. Karan D, Chen S-J, Johansson SL, Singh AP, Paralkar VM, Lin M-F et al. Dysregulated expression of MIC-1/PDF in human prostate tumor cells. *Biochem Biophys Res Commun* 2003; **305**: 598–604.
43. Senapati S, Rachagani S, Chaudhary K, Johansson SL, Singh RK, Batra SK. Overexpression of macrophage inhibitory cytokine-1 induces metastasis of human prostate cancer cells through the FAK-RhoA signaling pathway. *Oncogene* 2010; **29**: 1293–1302.
44. Zhou Y, Zhong Y, Wang Y, Zhang X, Batista DL, Gejman R et al. Activation of p53 by MEG3 Non-coding RNA. *J Biol Chem* 2007; **282**: 24731–24742.
45. Lim JH, Park J-W, Min DS, Chang J-S, Lee YH, Park YB et al. NAG-1 up-regulation mediated by EGR-1 and p53 is critical for quercetin-induced apoptosis in HCT116 colon carcinoma cells. *Apoptosis* 2007; **12**: 411–421.
46. Baek SJ, Kim KS, Nixon JB, Wilson LC, Eling TE. Cyclooxygenase inhibitors regulate the expression of a TGF-beta superfamily member that has proapoptotic and antitumorigenic activities. *Mol Pharmacol* 2001; **59**: 901–908.
47. Yamakuchi M, Ferlito M, Lowenstein CJ. miR-34a repression of SIRT1 regulates apoptosis. *Proc Natl Acad Sci USA* 2008; **105**: 13421–13426.
48. Hermeking H. The miR-34 family in cancer and apoptosis. *Cell Death Differ* 2009; **17**: 193–199.
49. Murphy M, Ahn J, Walker KK, Hoffman WH, Evans RM, Levine AJ et al. Transcriptional repression by wild-type p53 utilizes histone deacetylases, mediated by interaction with mSin3a. *Genes Dev* 1999; **13**: 2490–2501.
50. Juan LJ, Shia WJ, Chen MH, Yang WM, Seto E, Lin YS et al. Histone deacetylases specifically down-regulate p53-dependent gene activation. *J Biol Chem* 2000; **275**: 20436–20443.
51. Kasinski AL, Slack FJ. MicroRNAs en route to the clinic: progress in validating and targeting microRNAs for cancer therapy. *Nat Rev Cancer* 2011; **11**: 849–864.
52. Broderick JA, Zamore PD. MicroRNA therapeutics. *Gene Ther* 2011; **18**: 1104–1110.
53. Le MTN, Shyh-Chang N, Khaw SL, Chin L, Teh C, Tay J et al. Conserved regulation of p53 network dosage by microRNA–125b occurs through evolving miRNA–target gene pairs. *PLoS Genet* 2011; **7**: e1002242.
54. Edgar RC. MUSCLE: a multiple sequence alignment method with reduced time and space complexity. *BMC Bioinformatics* 2004; **5**: 113.
55. Altschul SF, Madden TL, Schäffer AA, Zhang J, Zhang Z, Miller W et al. Gapped BLAST and PSI-BLAST: a new generation of protein database search programs. *Nucleic Acids Res* 1997; **25**: 3389–3402.

56. Karolchik D, Barber GP, Casper J, Clawson H, Cline MS, Diekhans M *et al.* The UCSC Genome Browser database: 2014 update. *Nucleic Acids Res* 2014; **42**: D764–D770.

57. Tamura K, Peterson D, Peterson N, Stecher G, Nei M, Kumar S. MEGA5: molecular evolutionary genetics analysis using maximum likelihood, evolutionary distance, and maximum parsimony methods. *Mol Biol Evol* 2011; **28**: 2731–2739.

58. Stamatakis A, Aberer AJ, Goll C, Smith SA, Berger SA, Izquierdo-Carrasco F. RAxML-Light: a tool for computing terabyte phylogenies. *Bioinformatics* 2012; **28**: 2064–2066.

59. Ogurtsov AY, Shabalina SA, Kondrashov AS, Roytberg MA. Analysis of internal loops within the RNA secondary structure in almost quadratic time. *Bioinformatics* 2006; **22**: 1317–1324.

60. Lorenz R, Bernhart SH, Höner Zu Siederdissen C, Tafer H, Flamm C, Stadler PF *et al.* ViennaRNA Package 2.0. *Algorithms Mol Biol* 2011; **6**: 26.

Supplementary Information accompanies this paper on Cell Death and Differentiation website (http://www.nature.com/cdd)